ELSEVIER

Journal of Nuclear Materials 296 (2001) 174–182

journal of nuclear materials

www.elsevier.com/locate/jnucmat

Microstructure of both as-irradiated and deformed 304L stainless steel irradiated with 800 MeV protons

Y. Dai [a,*], X. Jia [a], J.C. Chen [b], W.F. Sommer [c], M. Victoria [d], G.S. Bauer [a]

[a] *Spallation Neutron Source Division, Paul Scherrer Institut, Villigen PSI CH-5232, Switzerland*
[b] *Institut fur Festkoperforschung, Forschszentrum Julich, 52425 Julich, Germany*
[c] *MS H838, Los Alamos Neutron Science Center, Los Alamos National Laboratory, Los Alamos NM 87545, USA*
[d] *Fusion Technology Materials, CRPP, Ecole Polytechnique Federal de Lausanne, 5232 Villigen PSI, Switzerland*

Abstract

A 304L stainless steel water degrader was irradiated with 800 MeV protons at Los Alamos Neutron Science Centre (LANSCE) up to 8.5 dpa at temperatures up to 250°C. Tensile tests showed that hardening and embrittlement were induced in the material. In order to understand the irradiation hardening and embrittlement mechanism, the microstructure in both as-irradiated and deformed material has been studied. The results of TEM investigations show that in the as-irradiated material the main features are: (a) very dense small defect clusters, part of them can be resolved as stacking fault tetrahedra (SFT), with a mean size of about 1.6 nm independent of irradiation dose; (b) large Frank loops, whose size increases with dose but whose density varies little with dose; (c) amorphization of precipitates; and (d) no observable helium bubbles or cavities. The main feature in the deformed material is the formation of twin lamellae and bundles of twin lamellae. In all of the four samples (0, 0.7, 3.4 and 6.8 dpa) studied, dense twin lamellae have been observed. The twin planes are {1 1 1}. Similar to channels observed in irradiated and deformed fcc pure metals, the original microstructures inside the twin lamellae, namely small clusters and Frank loops, have been removed. The width of the twin lamellae and their bundles varies from a few nanometers to more than 100 nm. The structure outside the twin lamellae is little changed.

1. Introduction

Significant hardening and reduction of ductility can occur in metallic alloys as a result of high energy particle irradiation. This becomes a particular concern for high power spallation targets, because the degradation of material properties by radiation damage will be the most problematic factor in determining the efficiency and lifetime of target components [1,2].

In the materials R&D program for the European Spallation Sources (ESS), martensitic stainless steel and/or austenitic stainless steels have been chosen as candidate materials for the liquid metal container and the safety hull. As a part of the effort to establish a database for the ESS engineering design, a spent 304L stainless steel water degrader from Los Alamos Neutron Science Centre (LANSCE), which was irradiated with 800 MeV protons up to a displacement damage level of about 8.5 dpa, has been investigated jointly by Forschungszentrum Jülich (FZJ) in Germany and the Paul Scherrer Institut (PSI) in Switzerland [3]. The results of tensile tests performed at room temperature showed that significant irradiation hardening occurred at a dose as low as 0.3 dpa. The irradiation hardening increased with increasing irradiation dose, the ductility of the materials substantially decreased, by 50% at 0.3 dpa and 90% at 8 dpa. To understand the irradiation hardening and embrittlement effects, it is necessary to investigate the microstructure in both as-irradiated and deformed materials. There are only few reports in the literature about the microstructure in austenitic stainless steels irradiated in the low temperature regime, $T < 300$°C. The present work gives more detailed information of the microstructure in both as-irradiated and deformed materials.

* Corresponding author. Tel.: +41-56 310 4171; fax: +41-56 310 2485.
E-mail address: yong.dai@psi.ch (Y. Dai).

0022-3115/01/$ - see front matter
PII: S0022-3115(01)00565-7

2. Experimental

The detailed information describing the LANSCE water degrader and the irradiation can be found in [3] so only a brief description is given here.

Part of the water degrader is a commercial type of AISI 304L stainless steel. The exact heat treatment and composition of the material is not known since no original material is available. For the control tensile test, a piece of 304L is used. The nominal composition for 304L is: 17–20 Cr wt%, 10–12.5 wt% Ni, <2.0 wt% Mn, <1.0 wt% Si, and P, S, Cu, N and C below 0.5 wt% in sum, and Fe balance.

The irradiation temperature was below 250°C. The proton fluence distribution was determined from gamma-scans [4]. The maximum fluence of about 2.9×10^{25} p/m^2 was obtained, which corresponded to a damage dose of about 8.5 dpa. Tensile tests were performed at room temperature [3]. The results are listed in Table 1.

Transmission electron microscopy (TEM) samples of 1.0 mm diameter were used in the present study so that the microstructure in the deformed samples of 1.2 mm wide gauge part can be investigated. The small size of the TEM samples is also preferable since it reduces the activity of the samples significantly and, therefore, the very active samples are much easier to handle.

TEM samples of undeformed material were punched from the heads of deformed tensile specimens both unirradiated and irradiated to 0.7, 3.4 and 6.8 dpa, which were previously investigated by Chen et al. [3]. In addition, another two as-irradiated samples at 4.6 and 7.0 dpa were also observed. For deformed materials, the TEM samples were punched from the gauge areas of above deformed tensile samples, which had been strained to 83%, 45%, 12.5% and 7.4% elongation, respectively. After punching, these 1.0 mm diameter discs were then embedded in 3 mm diameter discs with 1.0 mm diameter holes at the centre. Afterwards, they were polished electrochemically in a Tenupol with a solution of 5 vol.% perchloric acid and 95 vol.% ethanol at −20°C and 60 V.

The TEM observation was performed in a JEOL 2010 type transmission electron microscope equipped with an EDX analysis system and operated at 200 keV. The most often used image conditions were bright field (BF) and weak beam dark field (WBDF) at $(g, 4g)$ or $(g, 5g)$, $g = 200$, or $g = 111$. Different magnifications were used depending on the objects observed. For observing small defect clusters a magnification of 200k times or higher was applied. To obtain quantitative information, the defect clusters and Frank loops were counted and measured from several pictures which were taken from different areas of each sample under the weak beam dark field condition $(g, 5g)$, $g = 200$ and $B \cong 110$. Generally, for each sample, more than 300 small clusters and 100 Frank loops were measured to get the size distribution and the mean size.

3. Results

3.1. Microstructure in undeformed materials

The microstructure in the reference 304L material at as-received condition is shown in Fig. 1(a). Dislocations are faulted and with an extension of few nm to hundreds nm between two partial dislocations. Large stacking fault tetrahedra (SFT) were seldom observed. After irradiation to a dose of 0.7 dpa or higher the original microstructure changed completely. Fig. 1(b) shows the situation at 0.7 dpa. It can be seen that very dense small defect clusters and some faulted Frank interstitial loops (stick like) have been introduced by irradiation. Some of the small clusters have clearly a triangle shape, which are SFT. With the irradiation dose increasing to 3.4 dpa, the density and size of small defect clusters show no obvious changes. For Frank loops, the size increases evidently, while the density is also little changed, see Fig. 1(c).

Table 1
Tensile results of 304L stainless steel irradiated with 800 MeV protons and tested at room temperature

Dose (dpa)	Yield stress (MPa)	Ultimate tensile strength (MPa)	Uniform elongation (%)	Total elongation (%)
0[a]	210	585	71	83
0.2	506	689	52	60
0.7[a]	530	705	38	45
1.5	583	725	37	43
3.3	713	805	29	37
3.4[a]	765	818	9.7	12.5
5.8	790	841	~10	12.5
6.8[a]	825	853	6.4	7.4
7.9	795	840	~11	13

[a] The samples are studied in the present work.

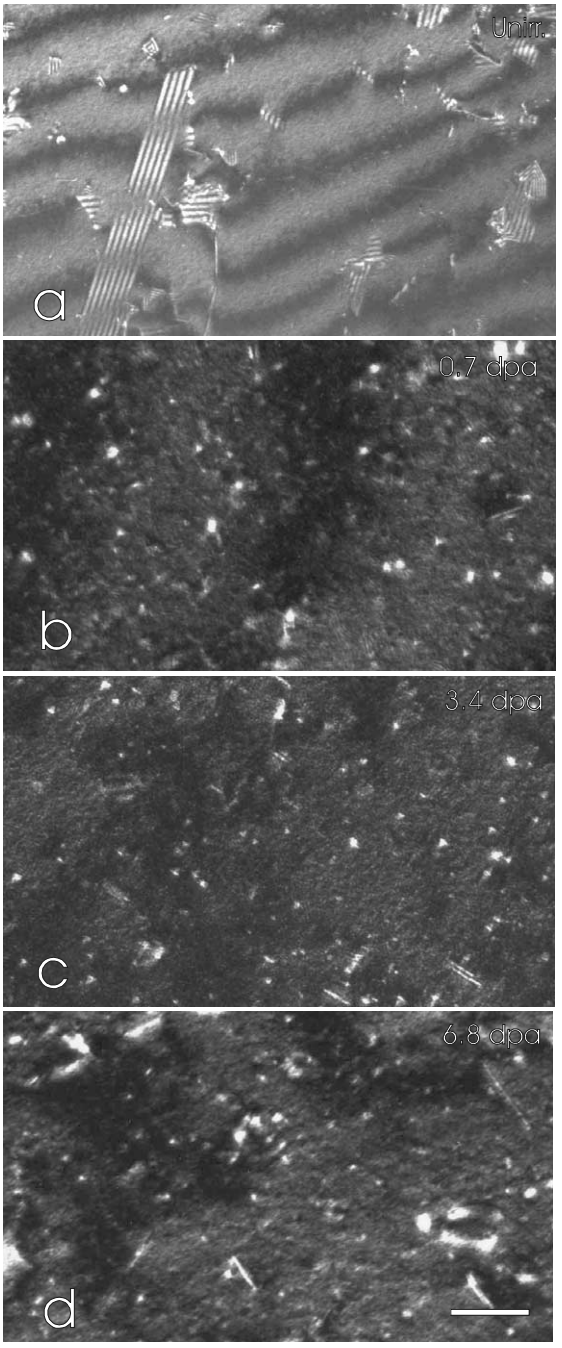

Fig. 1. WBDF graphs showing the microstructure in samples: (a) unirradiated; and (b)–(d) irradiated at 0.7, 3.4, and 6.8 dpa, respectively. The scale at right-lower corner of (d) represents 80 nm for graph (a) and 20 nm for the others.

When the dose reaches 7.0 dpa, the density and size of small defect clusters as well as the density of Frank loops remains essentially the same as at the lower doses, only the size of the Frank loops has greatly increased, as shown in Fig. 1(d).

The detailed information of the density and size of small clusters, Frank loops and SFT is given in Table 2 and also plotted in Fig. 2. It can be seen that the size of defect clusters (including SFT) is very small with a mean size of about 1.6 nm, which remains almost constantly at all doses. The mean size of resolvable SFT is about 1.5 nm, which is also insensitive to the irradiation dose. The density of SFT is about 20–25% of the total small cluster density. For Frank loops, the mean size increases quickly from 3.9 nm at 0.7 dpa to 7.8 nm at 3.4 dpa and up to about 20 nm at 7.0 dpa, while the density of Frank loops changes little in the same dose range. Since the thickness of the thin foils was deduced from the number of fringes, the uncertainty of the given densities is estimated to be about $\pm 15\%$.

The size distributions of the small clusters and SFT are illustrated in Fig. 3(a), and of Frank loops are given in Fig. 3(b). The size distributions of small clusters and SFT look similar for all doses. However those of Frank loops clearly shift to larger sizes with increasing dose. The small clusters have a size normally below 5 nm while SFT remain below 3 nm. The Frank loops have sizes up to 50 nm at high doses.

The density of precipitates is low in this 304L stainless steel. They are mostly located at grain boundaries and have sizes up to hundreds of nm. EDX analysis results show that the precipitates are rich in Cr ($\sim$67%) and Fe ($\sim$27%), with low Mn, Ni, V and Si contents. The diffraction patterns indicate that they are $M_{23}C_6$ type. At higher doses, there is no noticeable change in the composition, but the crystal structure of these precipitates has changed from crystalline at lower dose (0.7 dpa, Fig. 4(a)) to amorphous at higher dose (3.4 dpa and higher, Fig. 4(b)).

3.2. Microstructure in deformed materials

The microstructure in deformed reference samples is illustrated in Fig. 5. At a large deformation level of 83%, dislocation networks have been well established as shown in Fig. 5(a), which is similar to that generally observed in deformed stainless steels. Fig. 5(b) presents a picture of an area where there are dense twin lamellae and bundles of twin lamellae. The diffraction pattern taken from the area is given at the upper-right corner, which indicates clearly that the twin planes are {1 1 1}. The width of the twin lamellae can be as small as few nanometers but that of the bundles can be as large as hundreds of nanometers. There are very few dislocations and no dislocation pile-ups observed inside the twin lamellae. However, in some cases there are very dense dislocations located at the two sides of a twin lamella, as shown in Fig. 5(c).

Table 2
Summary of the size distribution and density of clusters of 304L Stainless Steel irradiated with 800 MeV protons

Dose (dpa)	Small cluster		Frank loop		SFT	
	Mean size (nm)	Density (10^{22} m^{-3})	Mean size (nm)	Density (10^{22} m^{-3})	Mean size (nm)	Density (10^{22} m^{-3})
0.7	1.7	3.5×10^{23}	3.9	7.6×10^{22}	1.5	6.2×10^{22}
3.4	1.6	3.7×10^{23}	7.8	7.9×10^{22}	1.5	1.0×10^{23}
4.6	1.6	3.7×10^{23}	12.8	1.2×10^{23}	1.4	6.7×10^{22}
6.8	1.6	4.2×10^{23}	17.4	5.3×10^{22}	1.5	6.0×10^{22}
7.0	1.6	4.3×10^{23}	19.9	8.0×10^{22}	1.5	9.8×10^{22}

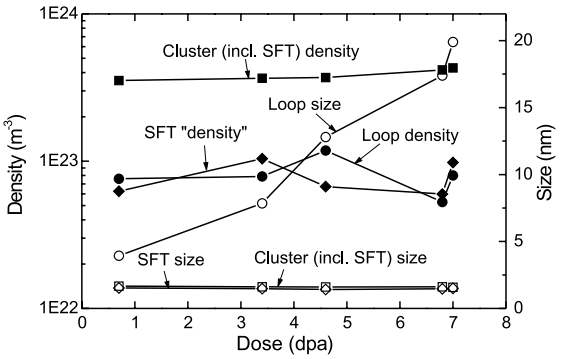

Fig. 2. Irradiation dose dependence of the densities and sizes of small defect clusters (including SFT), SFT and Frank loops.

The main features of the microstructure in irradiated and deformed samples are the formation of dense twin lamellae, as shown in Figs. 6(a)–(c) for the cases at 0.7, 3.4 and 6.8 dpa, respectively. The difference in the twin structure in the different cases, including the reference sample (5(b)), is not so straightforward. There is no evident irradiation dose dependence of the width and density of twin lamellae and their bundles.

Actual measurements on the micrographs show that the deformation is concentrated in twin lamellae. This can be seen clearly in Fig. 7, which demonstrates the situation at the intersection of twin lamellae on two different {1 1 1} planes. In this dark-field image picture, due to the imaging condition, the twin lamella indicated by arrows has no contrast, while the four lamellae on intersecting {1 1 1} plane have strong bright images. From the displacement between the lower and upper parts of the four edge-on twin lamellae, it is estimated that at least 80% of strain is located in the indicated twin lamella.

In order to have a clear picture of twin lamellae, stereo pairs have been taken. An example is given as Fig. 8 which shows a small volume with a number of

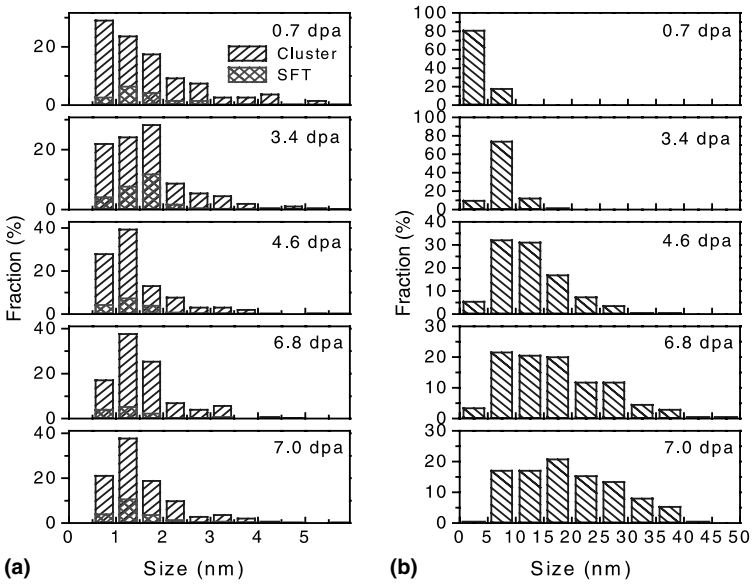

Fig. 3. The size distributions for (a) small defect clusters (including SFT) and SFT, and (b) Frank loops.

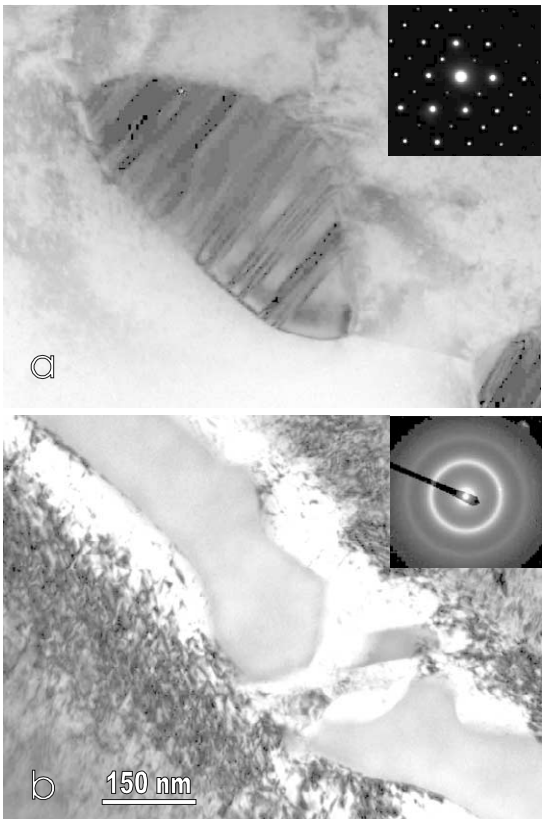

Fig. 4. Micrographs showing precipitates in samples of (a) 0.7 dpa and (b) 3.4 dpa. The diffraction pattern in each graph was taken from the corresponding precipitates. Notice the structure of the precipitates changes from crystalline to amorphous when the dose increases from 0.7 to 3.4 dpa.

twin lamellae on, actually, two sets of {1 1 1} planes. Under a stereo-viewer it can be seen that all the visible twin lamellae are thin slices. The invisible twin lamellae (indicated by arrows) seem quite similar. The visible lamellae presumably formed first and were then intersected by the invisible ones, since the later are straight and the former are zigzag like. It is clear that the displacement induced by the invisible twin lamellae is as large as several tens of nanometers.

Similar to the channelling phenomena observed in deformed irradiated FCC pure metals such as Cu and Pd, twin lamellae and their bundles form also plenty of 'defect-free' channels in the irradiated 304L samples during deformation. In fact, there are almost no small defect clusters and large faulted Frank loops in these channels, as shown in Fig. 9. Again, there is essentially no change in the microstructure outside the channels.

Special attention has been given to the determination of how twin lamellae interact with grain boundaries.

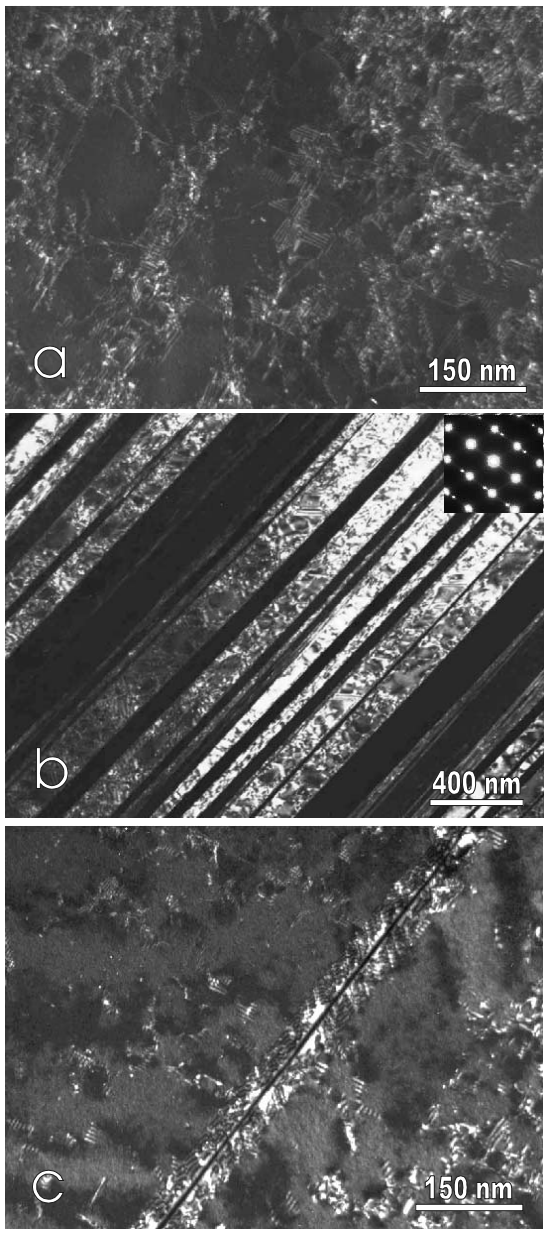

Fig. 5. Microstructure in an unirradiated sample after 83% deformation, (a) showing the dislocation structure, (b) and (c) showing the twin lamellae.

Within the small volume of all the samples observed, there are only few grain boundaries visible. Unlike the relatively simple picture of the interaction between twin lamellae, the interaction between twin lamellae and grain boundaries looks complicated. There is some evidence showing that grain boundaries are not as smooth as before and become somewhat distorted as shown in Fig. 10.

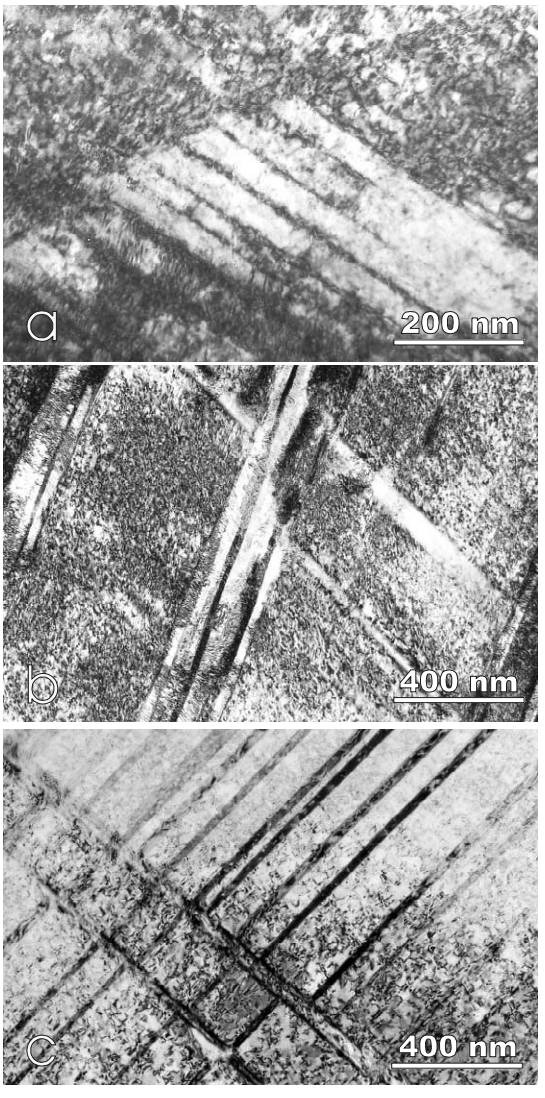

Fig. 6. Micrographs showing the twin structure in deformed samples: (a) 0.7 dpa, (b) 3.4 dpa and (c) 6.8 dpa.

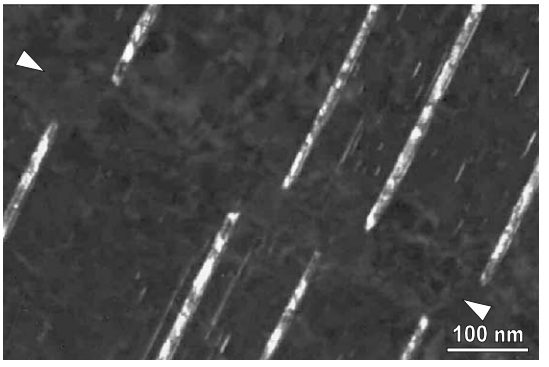

Fig. 7. A micrograph showing the interaction between twin lamellae on different {1 1 1} planes. Notice the displacement induced by the twin indicated by the arrows on the other four twins (edge-on).

4. Discussion

4.1. Microstructure in as-irradiated samples

Austenitic stainless steels such as types 304 and 316 are widely used as structural materials in nuclear reactors. They are also the tentative candidate materials for the fusion reactor first wall. Because of this, irradiated austenitic steels have been studied intensively in the last decades. However, the mechanical behaviour and microstructures of austenitic steels after irradiation in the low temperature regime ($T_i \leqslant 300$°C, $\sim 0.3\ T_m$, T_m is melting temperature) has not been well studied. Nevertheless there are still a number of cases [5–13] where the microstructure of 316 or 304 stainless steels have been studied after irradiation at temperatures below 300°C.

The general features of the microstructure observed by different investigations are very similar, namely very dense small defect clusters with or without faulted Frank loops, depending on the dose level. To compare the data of the present work with the published data, a summary of the data from [5,6,11–13] on annealed 316 and 304 irradiated to doses $\geqslant 0.5$ dpa is given in Fig. 11. For small defect clusters, the density and size have been quantified in [5,6,12] and only few data are available. It can be seen that the density of small clusters saturates at a level between 2×10^{23} and 4×10^{23} m^{-3} at doses above 0.5 dpa and the mean size is about 1.5–2 nm, independent of the dose. The reason for the data at 7.3 dpa given by Wiffen et al. deviate from the other data could be that the quality of TEM was not good enough at that time (1981) and very small clusters might not be resolved and, therefore, showed a larger mean size and a lower density. Although fully quantitative information was not given, it was mentioned by Lee et al. [10] that the density of black dots was estimated to saturate at $2\text{–}4 \times 10^{23}$ m^{-3} in AISI 316LN irradiated with He^+ or Fe^+ at a dose level between 0.1 and 1 dpa. In samples irradiated at 90°C, Yoshida [7] found that the density of small clusters increased from about 4×10^{23} to 2.5×10^{24} m^{-3} when the dose increased from 0.001 to 0.032 dpa. These values are much higher than the data shown in Fig. 11(a) at higher doses.

For faulted Frank loops, the density measured by different authors is very scattered and has a variation of almost a factor of 10, as shown in Fig. 11(a). The data on the size of Frank loops have a much better correlation (Fig. 11(b)) except those of Bailat et al. [11]. The higher density and much smaller size obtained by Bailat et al. at 7.5 dpa may be because defect clusters and Frank loops might not be well separated. One reason for

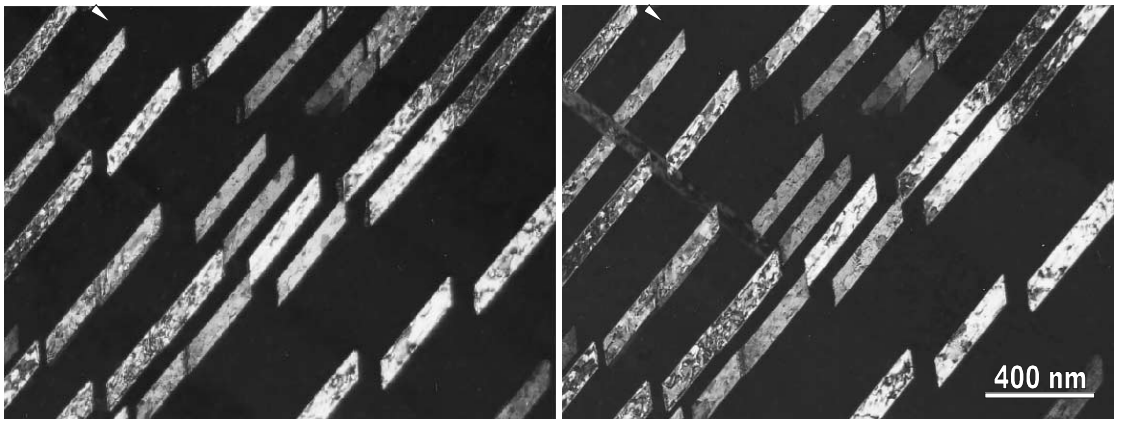

Fig. 8. A stereo pair of DF images showing the twin lamellae formed in the sample of 6.8 dpa.

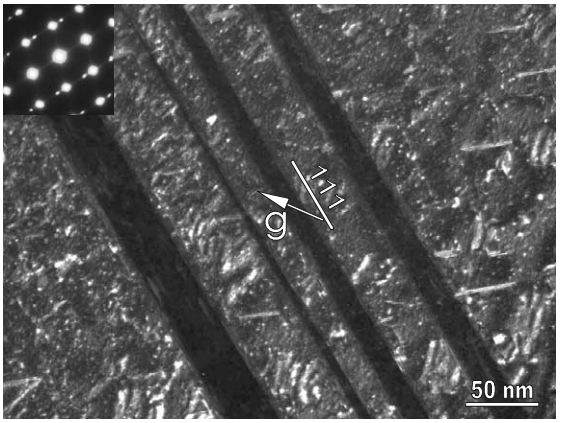

Fig. 9. WBDF image showing twin lamellae in the sample of 6.8 dpa.

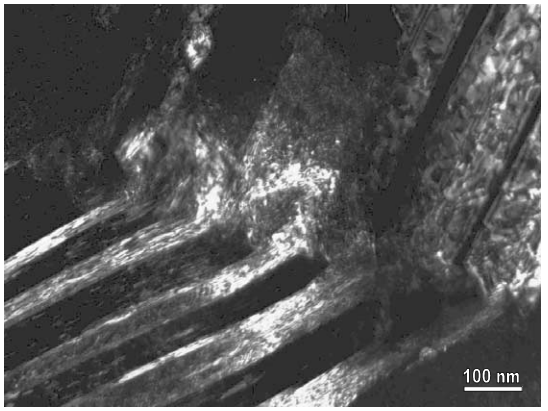

Fig. 10. DF image showing the interaction between twin lamellae and a grain boundary in the sample of 6.8 dpa.

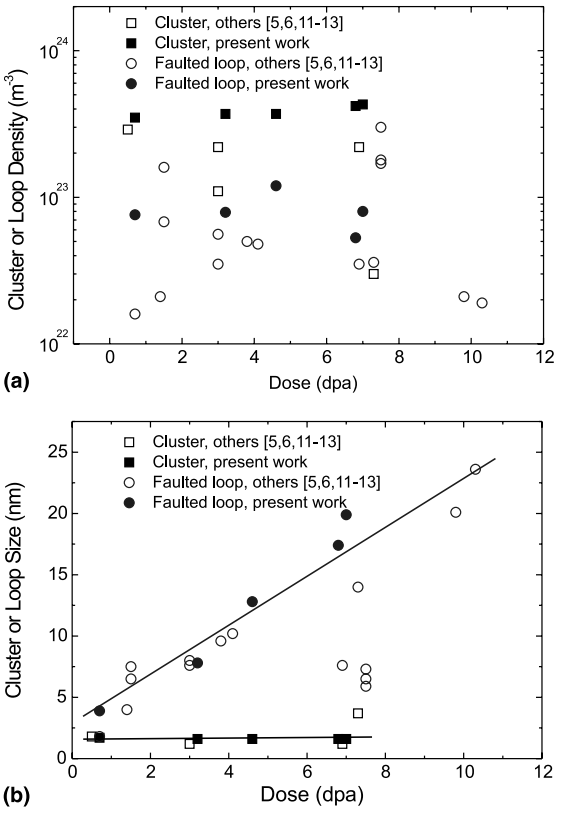

Fig. 11. Dose dependence of (a) the densities of defect clusters and Frank loops, (b) the sizes of defect clusters and Frank loops for stainless steels 316 and 304 irradiated at low temperature regime.

the overall large variation could be the irradiation temperature effects as noticed by Maziasz [8] and Hashimoto et al. [12]. Nevertheless, it is clear that the size

of Frank loops increases more or less linearly with increasing dose in this dose range at temperatures below 300°C.

It is also noticed that the data on the size of Frank loops obtained by Maziasz [8] in cold worked PCA at 7.4 dpa and obtained by Wiffen and Maziasz [5] in cold worked 316 at 10.8 dpa agree with other data very well. The density of Frank loops are much lower in cold worked samples irradiated at 55–60°C, but in the sample irradiated at 200°C it is more or less as high as in annealed samples.

In general the data of the present study agree well with the published data. The density of defect clusters in this study is systematically a little higher than the published data. This could be because the defect clusters were counted from thin areas between 20 and 30 nm thick while other authors (e.g., [6,12]) generally counted them from areas of 50–100 nm thick. The authors noticed that, due to the increasing overlap of the images and the decreasing visibility of very small ones, the number density of defect clusters decreases continuously when the thickness of the area increases from a starting thickness of about 30 nm.

One of the most interesting results of the present study is that a large number of SFT have been observed in all of samples in the dose range from 0.7 to 7 dpa. The SFT have a mean size of about 1.5 nm and a density of $6–10 \times 10^{22}$ m^{-3}, corresponding to 20–25% of the total small clusters. Both the size and the density of the SFTs are insensitive to the dose.

Since stainless steels such as 316 and 304 have a low stacking fault energy, SFT should be the preferred form of the small defect clusters produced by irradiation in low temperature regime ($T \leqslant 0.3\ T_m$) [14]. However, SFT in stainless steels are not observed as readily as in pure fcc metals such as Cu and Au even though the stacking fault energy of Cu is much higher. The main reason, as often mentioned in the literature, could be that the defect clusters (including SFT) in irradiated stainless steels are too small to determine their morphology if the effective resolution of a microscope is not good enough. The second reason could be that the surface condition of an irradiated stainless steel TEM sample is generally poor for high resolution observations and this makes the observation of SFT very difficult. Nevertheless, Zinkle et al. [6] performed successful observations and showed that there were SFTs formed in neutron irradiated 304L, although the SFTs were only 0.2% of the total defect clusters.

Since the irradiation temperature is low, $<0.3\ T_m$, segregation processes enhanced by irradiation should be slow. Consequently, the initial precipitate structures should be difficult to change and new precipitate phases should be difficult to form. This may be the reason why no changes in the composition and morphology of the precipitates have been observed. However, as in the case in martensitic steels irradiated in the low temperature regime [2,15], the irradiation-induced amorphization of precipitates has been also observed in 304 SS starting at similar dose, between 0.7 and 3.4 dpa.

Recent measurements show that 800 MeV proton irradiation produces about 180 appm He per dpa in stainless steels [16]. This means in the sample of 7 dpa the He concentration is about 1260 appm. But at the present irradiation temperatures He bubbles are probably still too small to be resolved.

The tensile test results showed that the yield stress increased about by 320, 560 and 620 MPa for the samples of 0.7, 3.4 and 6.8 dpa, respectively. Using the data for the density and size of defects for these three samples and using values 0.15 and 0.5 for the barrier strength of defect clusters and Frank loops [12], it is calculated that the increments of yield stress are about 340, 480 and 570 MPa for the three samples, respectively. For samples at 3.4 and 6.8 dpa, the calculated values are lower than the measured ones. It may indicate that helium contributes the additional hardening. This should not be surprising since there are about 610 and 1260 appm helium in these two samples, respectively. The helium effects, namely the contribution to hardening and stabilizing vacancy clusters, will be systematically investigated in future.

4.2. Microstructure in irradiated samples after deformation

In irradiated or quenched fcc pure metals such as Al, Cu, Au and Pd, dislocation channelling is often observed after deformation at low temperatures [17–20]. It has been observed that the small clusters produced by irradiation or quenching are almost completely removed in the channels. These channels are, therefore, called as 'defect-free' channels. However the 'defect-free' channels are not 'dislocation-free' channels. Random glide dislocations or even some dislocation tangles are often observed in the channels.

Recently, similar phenomena have been observed in stainless steels after irradiation and deformation at low temperatures [9,11,12,21]. In samples deformed at the room temperature it is found that the channels are, in fact, twin lamellae. Most of the observations [9,11,12] showed that inside the twin lamellae the radiation-induced defect clusters and Frank loops were removed. The present observation demonstrates the same features, namely the twin lamellae and their bundles are 'defect-free' zones, although some dislocations are also observed there.

An interesting observation is the similar twin structure in unirradiated samples after deformation. Although slip bends have been observed on the surfaces of unirradiated stainless steel specimens, twin lamellae are not readily observed. The formation of twin lamella in

the present unirradiated samples should be attributed to the high deformation level (83% elongation) [22].

The degradation of the mechanical properties of heavy irradiated materials may be associated with localized deformation. It is expected that there is a large stress concentration at the points of dislocation channels or twins intersecting at grain boundaries, which may initiate microcracks at grain boundaries and further lead to brittle fracture of the samples, or at least, substantial reduction of the ductility [11,23]. The distortion of grain boundaries observed in the present work (Fig. 10) may be an implication. Further delicate direct observations on the interaction of channels or twins with grain boundaries are planned.

5. Conclusion

The microstructure in deformed and undeformed 304L stainless steel irradiated with 800 MeV protons at temperature below 250°C have been investigated. The results obtained from unirradiated samples and irradiated samples of doses from 0.7 to 7 dpa show that:

1. The microstructure in the as-irradiated material can be characterized as irradiation-induced small defect clusters and faulted Frank loops. About 20% of the small defect clusters can be resolved as SFT.
2. In the dose range investigated, the densities of both small clusters and Frank loops are insensitive to the irradiation dose. The sizes of small clusters (including SFT) and SFT are about 1.6 and 1.5 nm, respectively, which are independent of the dose. The size of Frank loops is larger than that of clusters and more or less proportional to the dose, reaching a mean size of 20 nm at 7 dpa.
3. Pre-existing precipitates changed from crystalline to amorphous with increasing dose, and no helium bubbles or cavities were observed at all doses.
4. The main feature in the deformed samples is the formation of dense twin lamellae and bundles of twin lamellae parallel to $\{1\,1\,1\}$ planes. The width of the twin lamellae can be as small as few nanometers but that of bundles can be as large as hundreds of nanometers. The original existing microstructure (defect clusters and Frank loops) is almost completely removed in the twin lamellae but little changed in the blocks between the lamellae.
5. Due to the saturation of small defect clusters, further hardening at doses above about 0.5 dpa should be mainly attributed to Frank loops. Helium may have some contribution at high dose cases.

Acknowledgements

The great efforts of the members at the hot-labs in both FZJ and PSI to realize this work are highly acknowledged. We would also thank Dr R. Schäublin for his useful discussion and help on TEM observation and Dr K. Farrell for his useful comments. This work is partly supported by ESS TMR programme.

References

[1] ESS – A Next Generation Neutron Source for Europe, vol. 1–3, ESS Council 1997, ISBN 090 2376 500.
[2] Y. Dai, G.S. Bauer, F. Carsughi, H. Ulmaier, S.A. Maloy, W.F. Sommer, J. Nucl. Mater. 265 (1999) 203.
[3] J. Chen, Y. Dai, F. Carsughi, W.F. Sommer, G.S. Bauer, H. Ulmaier, J. Nucl. Mater. 275 (1999) 115.
[4] F. Carsughi, W.F. Sommer, H. Ulmaier, J. Nucl. Mater. 276 (2000) 289.
[5] F.W. Wiffen, P.J. Maziasz, J. Nucl. Mater. 103&104 (1981) 821.
[6] S.J. Zinkle, R.L. Sindelar, J. Nucl. Mater. 155–157 (1988) 1196.
[7] N. Yoshida, J. Nucl. Mater. 174 (1990) 220.
[8] P.J. Maziasz, J. Nucl. Mater. 191–194 (1992) 701.
[9] J.I. Cole, S.M. Brummer, J. Nucl. Mater. 225 (1995) 53.
[10] E.H. Lee, J.D. Hunn, T.S. Byun, L.K. Mansur, J. Nucl. Mater. 280 (2000) 18.
[11] C. Bailat, A. Almazouzi, N. Baluc, R. Schäublin, F. Gröschel, M. Victoria, J. Nucl. Mater. 283–287 (2000) 446.
[12] N. Hashimoto, S.J. Zinkle, A.F. Roweliffe, J.P. Robertson, S. Jitsukawa, J. Nucl. Mater. 283–287 (2000) 528.
[13] S.H. Sencer, G.M. Bond, F.A. Garner, M.L. Hamilton, S.A. Maloy, W.F. Sommer, these Proceedings, p. 145.
[14] S.J. Zinkle, L.E. Seitzman, W.G. Wolfer, Philos. Mag. A 55 (1987) 111.
[15] N. Baluc, R. Schäublin, C. Bailat, F. Paschoud, M. Victoria, J. Nucl. Mater. 283–287 (2000) 731.
[16] F.A. Garner, B.M. Oliver, L.R. Greenwood, M.R. James, P.D. Ferguson, S.A. Maloy, W.F. Sommer, these Proceedings, p. 66.
[17] M.S. Bapna, T. Mori, M. Meshii, Philos. Mag. 17 (1968) 177.
[18] T. Mori, M. Meshii, Acta Metall. 17 (1969) 167.
[19] Y. Dai, M. Victoria, MRS Symp. Proc. 439 (1997) 319.
[20] N. Baluc, C. Bailat, Y. Dai, M.L. Loppo, R. Schäublin, M. Victoria, MRS Symp. Proc. 540 (1999) 539.
[21] E.H. Lee, T.S. Byun, J.D. Hunn, K. Farrell, L.K. Mansur, these Proceedings, p. 183.
[22] A. Luft, Prog. Mater. Sci. 33 (1991) 97.
[23] Y. Chen, P. Spätig, M. Victoria, J. Nucl. Mater. 271&272 (1999) 128.